Terahertz Memos

Memo 04

August 2010

Investigation of the skin-effect losses in a copper SWO antenna above a copper ground plane

Prashanth Kumar[1], Carl E. Baum[1], Kenneth F. McDonald[2],
Christos G. Christodoulou[1] and Edl Schamiloglu[1]

[1]University of New Mexico
Department of Electrical and Computer Engineering
Albuquerque, NM 87131

[2]Sci-Eng Solutions, LLC
3304 Lake Town Dr.
Columbia, MO 65203

Abstract

This paper investigates the skin-effect losses in a copper Switched Oscillator (SWO) antenna above a copper ground plane. To quantify the resistive losses, the radiation quality factors for PEC and copper SWOs are compared using numerical simulations. An idealized switch is assumed.

1 Introduction

Having established that our numerical simulation software, CST MWS®, can reliably reproduce experimental data [1], we now proceed with the study and optimization of the Switched Oscillator (SWO) antenna [2]. The initial approach adopted here does not consider the physics of the photo-conductive-switch region (carrier lifetime, carrier mobility etc.). Nevertheless, the idealized (perfect) switch assumed in this paper provides valuable insight into the interdependence between various parameters of interest in the SWO design.

The skin-effect losses for the copper SWO antenna are investigated first. This is accomplished by comparing the radiation quality factors (Qs) for PEC and copper SWOs.

2 Determination of the input waveform

The input to the SWO antenna is a ramp rising step with a t_{mr} corresponding to the desired rise time. An ideal ramp rising input, as used in [2], is unsuitable for our simulations. This is because the sharp "knee" in such a waveform leads to inaccuracies at higher frequencies. Therefore, an input function which transitions smoothly from higher to lower frequencies is desired as it not only leads to more accurate simulations but also reduces the size of the simulation domain. One commonly used S-shaped function is the logisitic function, defined as

$$f(t) = \frac{a}{1 - b\exp(-ct)}, \tag{2.1}$$

where a, b and c are parameters. Recall that the t_{mr} is defined as,

$$t_{\mathrm{mr}} = \frac{f_{\mathrm{max}}}{(df/dt)_{\mathrm{max}}}. \tag{2.2}$$

As in [3], f_{max} is given in the limit $t \to \infty$, i.e., $f_{\mathrm{max}} = a$. The time τ at which (df/dt) is maximum is $\tau = \dfrac{\ln(b)}{c}$, therefore $(df/dt)_{\mathrm{max}} = \dfrac{ac}{4}$. The t_{mr} can now be easily estimated as

$$t_{\mathrm{mr}} = \frac{a}{\left[\frac{ac}{4}\right]} = \frac{4}{c} \tag{2.3}$$

A t_{mr} of 0.5 ps was found to lead to a reasonable number of mesh cells, i.e., $c = 4/t_{\mathrm{mr}} = 8$. The t_{mr} is independent of a and b. A plot of $f(t)$ is shown in Fig. 2.1.

3 Numerical simulations

3.1 Structure Visualization

Fig. 3.1 shows the perspective, top and side views of the SWO over a ground plane. The labeling conventions of [4] are adopted with a change in the orientation of the coordinate system. The SWO is designed with dimensions corresponding to a frequency of 0.5 THz, i.e., $\lambda = \lambda_0 = 600$ μm. There no substrate medium, i.e., vacuum between SWO and the ground plane. The dimensions of the setup are summarized in Table 1.

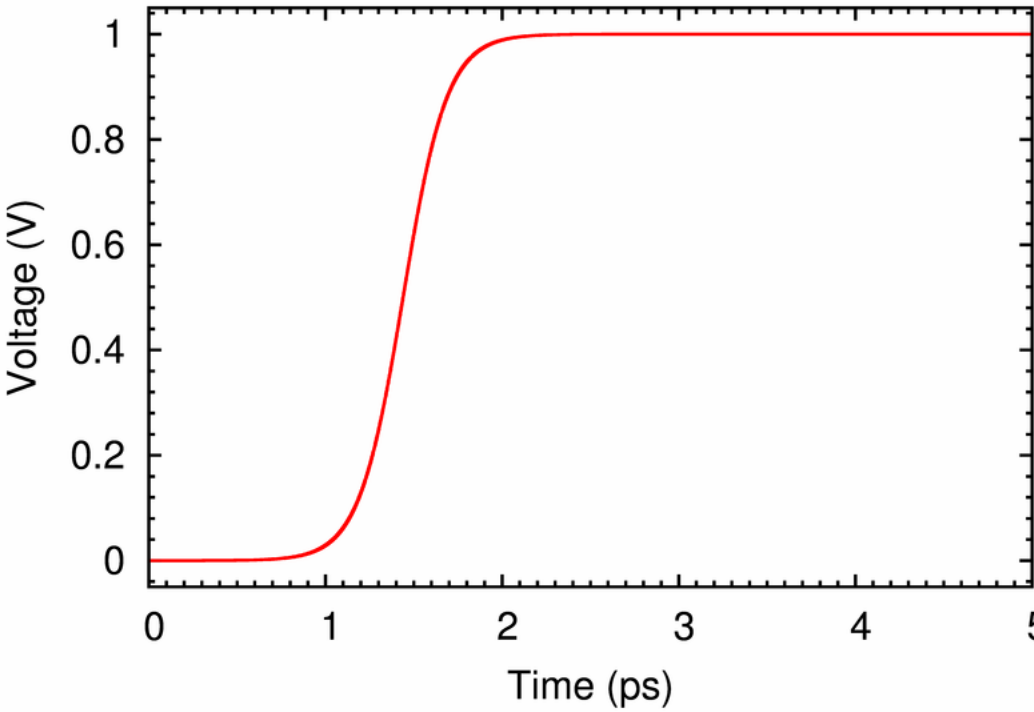

Figure 2.1: Logisitic input voltage waveform, with a t_{mr} of 0.5 ps, for the SWO antenna.

Table 1: Dimensions for a SWO over a ground plane and no substrate medium.

Parameter	Dimensions (μm)
Antenna length, l_a	$\lambda/2 = 300$
Antenna height (thickness)	$\lambda/600 = 1$
Switch length, l_s	$\lambda/50 = 12$
Antenna width, w	$(l_a - l_s)/2 = 144$
Height above ground plane, h	$\lambda/20 \leq h \leq \lambda/4$
Length of ground plane	$3\lambda = 1800$
Width of ground plane	$3\lambda = 1800$
Height of ground plane (thickness)	$\lambda/600 = 1$

3.2 Probe placements

Far-field electric-field probes were placed at 1 cm from the origin, along the z-axis, oriented in the x, y and z directions, as shown in Fig. 3.2.

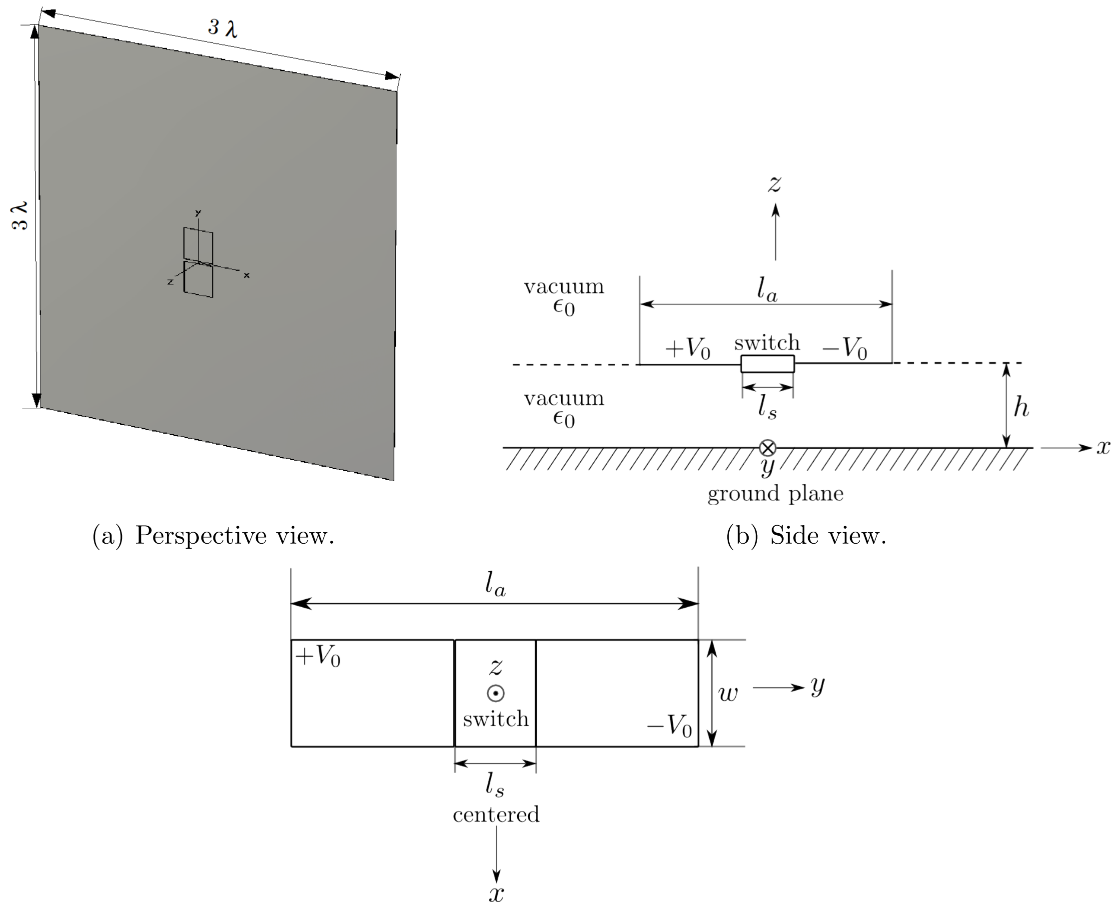

(a) Perspective view.
(b) Side view.
(c) Top view.

Figure 3.1: Perspective, top and side views of the SWO simulation setup.

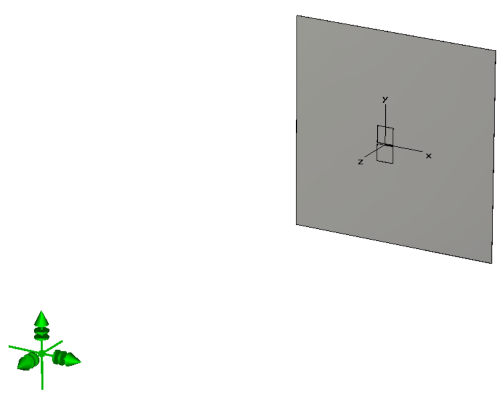

Figure 3.2: Orientations and placements of electric field probes.

3.3 Important CST/Simulation Parameters

Domain	Time
Excitation	Discrete
Input	Logistic (see Sec. 2)
Peak excitation voltage	1 V
Excitation duration	400 ps
Frequency range	0−4 THz
LPW	10

3.4 Results

Before proceeding to compare the quality factors for copper and PEC SWOs as a function of h, it is useful to compare the numerical simulation results with the analytical results in [4] for two (extreme) cases, $h = \lambda/4$ and $h \ll \lambda$. The analytical calculations assume a PEC SWO and PEC ground plane.

3.4.1 Q for a PEC SWO at a distance of $\lambda/4$ over a PEC ground plane ($h = \lambda/4$)

The far-field electric field in the time and frequency domains are shown in Fig. 3.3(a) and Fig. 3.3(b) respectively. As mentioned in [4], the oscillation is highly damped, Fig. 3.3(a). The SWO antenna resonates at a frequency of $f_0 = 0.321$ THz, Fig. 3.3(b). The Q, calculated from the 3 dB points in Fig. 3.3(b), is 7.012. The formula for radiation Q for $h = \lambda/4$ as derived in [4] is

$$Q \approx \frac{w[l_a - l_s]}{hl_a} \tag{3.1}$$

which for our simulation setup is $Q = 0.96$. One thus notes a large discrepancy between the analytical prediction and that obtained from our simulation. This could be due to the following simplifications in [4],

- The effect of the fringe fields on the radiated field are not taken into account.
- The dipole moment at the resonant frequency, $\widetilde{\vec{p}}(j\omega_0)$, is calculated by assuming a previously known current distribution.
- The theory assumes an ideal step input.

3.4.2 Q for a PEC SWO at a distance of $\lambda/20$ over a PEC ground plane ($h \ll \lambda$)

The far-field electric field in the time and frequency domains are shown in Fig. 3.4(a) and Fig. 3.4(b) respectively. As expected, the oscillations are much less damped compared to analogous results for $h = \lambda/4$, Fig. 3.4(a). The SWO antenna resonates at a frequency of 0.338 THz, Fig. 3.4(b). The Q, calculated from the 3 dB points in Fig. 3.4(b), is 84.803. The formula for radiation Q for $h \ll \lambda/4$ as derived in [4] is

$$Q \approx \frac{15}{64\pi}\left[\frac{l_a}{h}\right]^3 \tag{3.2}$$

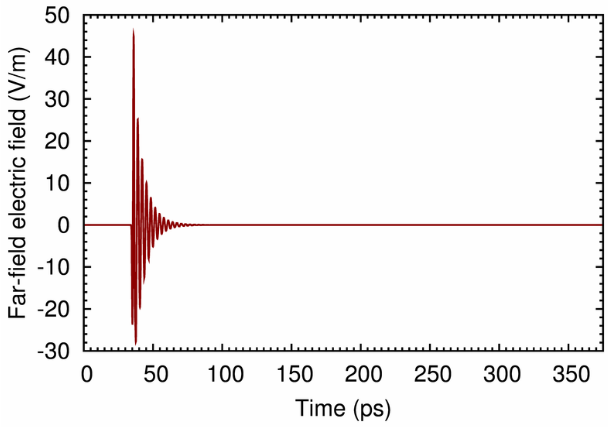

(a) Far-field electric field.

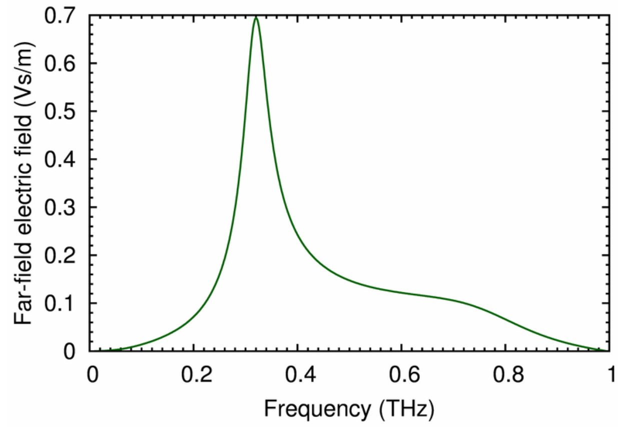

(b) Far-field electric field in the frequency domain (FFT of Fig. 3.3(a)).

Figure 3.3: Far-field electric field (from E_y probe) for the SWO $h = \lambda/4$ above the ground plane.

which for our simulation setup is $Q = 74.60$. One notes that the percentage deviation between the simulation and analytical prediction is much less for this case compared to $h = \lambda/4$.

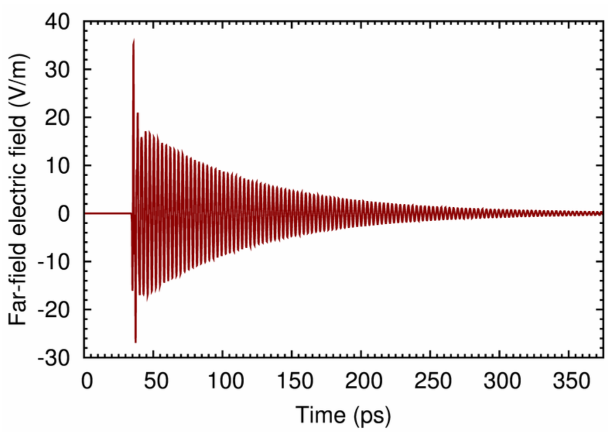

(a) Far-field electric field.

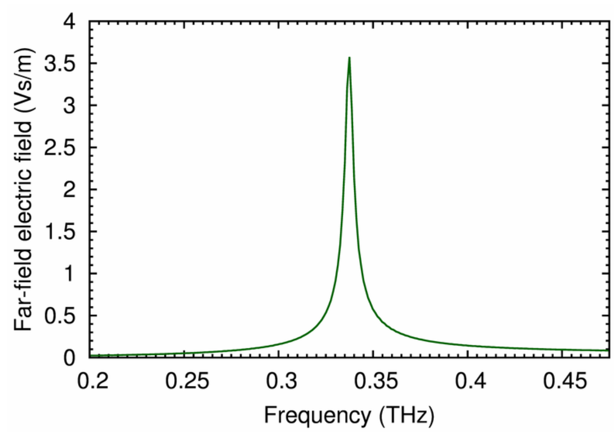

(b) Far-field electric field in the frequency domain (FFT of Fig. 3.4(a)).

Figure 3.4: Far-field electric field (from E_y probe) for the SWO $h = \lambda/20$ above the ground plane.

3.5 Comparison of Qs for PEC and Copper SWOs

Table. 2 summarizes the peak electric field ($E_{\max}$), resonant frequency (f_0) and quality factor (Q) as a function of the height of a PEC SWO above a PEC ground plane. The Q increases as h is decreased since more stored energy as the SWO is brought closer to the ground plane. One notes that there is little deviation in the resonant frequency compared to that in Q. The mean f_0 is 0.331 THz with a standard deviation of 0.0071.

Table 2: Variation of the peak electric field ($E_{\max}$), resonant frequency (f_0) and quality factor (Q) with the height of a PEC SWO above a PEC ground plane (h).

h/λ	$E_{\max}$ (V/m)	f_0 (THz)	Q
0.050	35.135	0.338	84.803
0.075	41.936	0.339	43.638
0.100	46.399	0.338	27.467
0.125	48.988	0.334	19.439
0.150	50.202	0.332	14.74
0.175	50.573	0.328	11.727
0.200	49.838	0.325	9.616
0.225	47.953	0.322	8.119
0.250	44.983	0.321	7.01

Table. 3 summarizes the peak electric field ($E_{\max}$), resonant frequency (f_0) and quality factor (Q) as a function of the height of a copper SWO above a copper ground plane (h). Again, one notes that there is little deviation in the resonant frequency compared to that in Q. The mean f_0 is 0.330 THz with a standard deviation of 0.0069, which is identical to the PEC case.

Table 3: Variation of the peak electric field ($E_{\max}$), resonant frequency (f_0) and quality factor (Q) with the height of a copper SWO above a copper ground plane (h).

h/λ	$E_{\max}$ (V/m)	f_0 (THz)	Q
0.050	34.793	0.336	56.805
0.075	41.521	0.339	36.14
0.100	45.964	0.337	24.824
0.125	48.57	0.334	18.179
0.150	49.779	0.33	14.072
0.175	50.154	0.327	11.303
0.200	49.441	0.325	9.399
0.225	47.607	0.322	7.98
0.250	44.698	0.32	6.891

The quality factor as a function of h for the PEC and copper cases are compared in Fig. 3.5. The analytical points, calculated in Sec. 3.4.1 and Sec. 3.4.2, for $h = \lambda/4$ and $h = \lambda/20$ are also indicated for reference. Such a comparison enables one to assess the effect of copper losses for various h. One observes that the resistive losses, R_s, are not a concern for $h \gtrapprox \lambda/10$. However, for $h \lessapprox \lambda/10$ the resistive losses significantly reduce the Q. Individual plots for the far-field electric field in the time and frequency domains for each data point in Fig. 3.5 are given in the appendix.

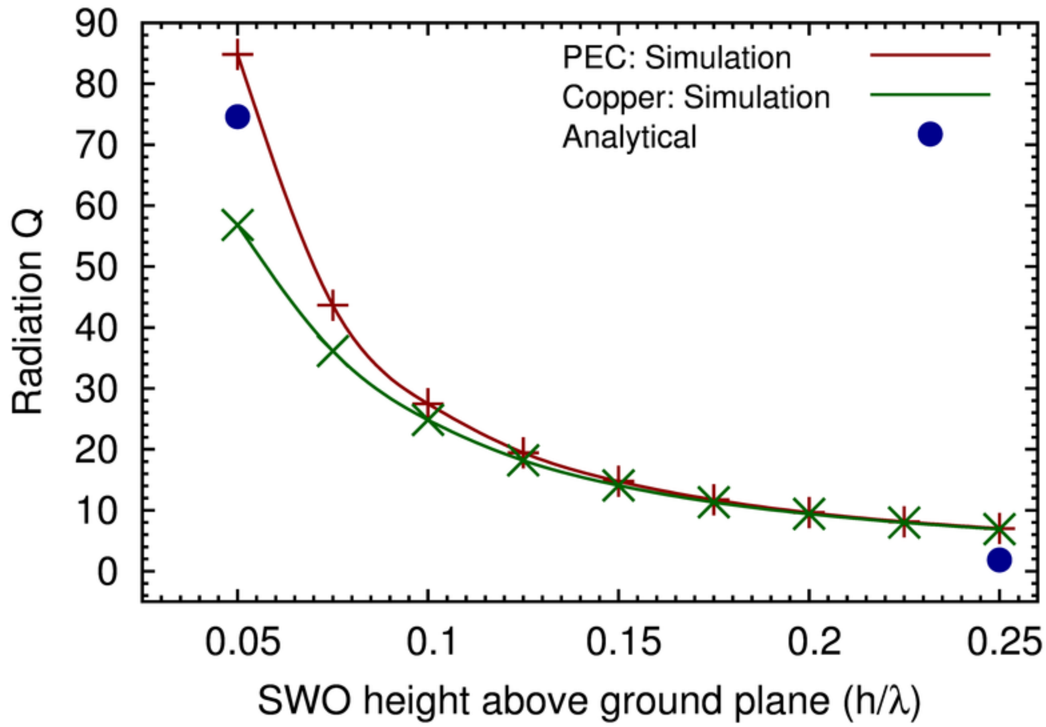

Figure 3.5: Comparison of the quality factors as a function of the SWO height above the ground plane for PEC and copper.

4 Conclusions

The Q increases as h is decreased, as expected. The losses due to the surface resistance of copper are not significant for $h \gtrapprox \lambda/10$, but for $\lessapprox \lambda/10$ the Q is lower than the corresponding results for PEC.

References

[1] Prashanth Kumar, Carl E. Baum, D. R. Grischkowsky, Kenneth F. McDonald, Christos G. Christodoulou and Edl Schamiloglu, “Comparison of experimental and numerical simulation results for the 5-10-5 max1 antenna,” *Terahertz Memo 3*, Aug. 2010.

[2] Prashanth Kumar, Carl E. Baum, Serhat Altunc, Christos G. Christodoulou and Edl Schamiloglu, “Switched oscillator as an antenna,” *Terahertz Memo 1*, Sept. 2009.

[3] C. E. Baum, “Some Considerations Concerning Analytic EMP Criteria Waveforms,” *Theoretical Note 285*, October 1976.

[4] C. E. Baum and P. Kumar, “Maximizing Energy in Terahertz Pulse Radiation from a Switched Oscillator,” *Sensor and Simulation Note XX*, July 2010.

Appendix

Radiated far-field electric fields, in the time and frequency domains, as a function of h for a copper SWO above a copper ground plane.

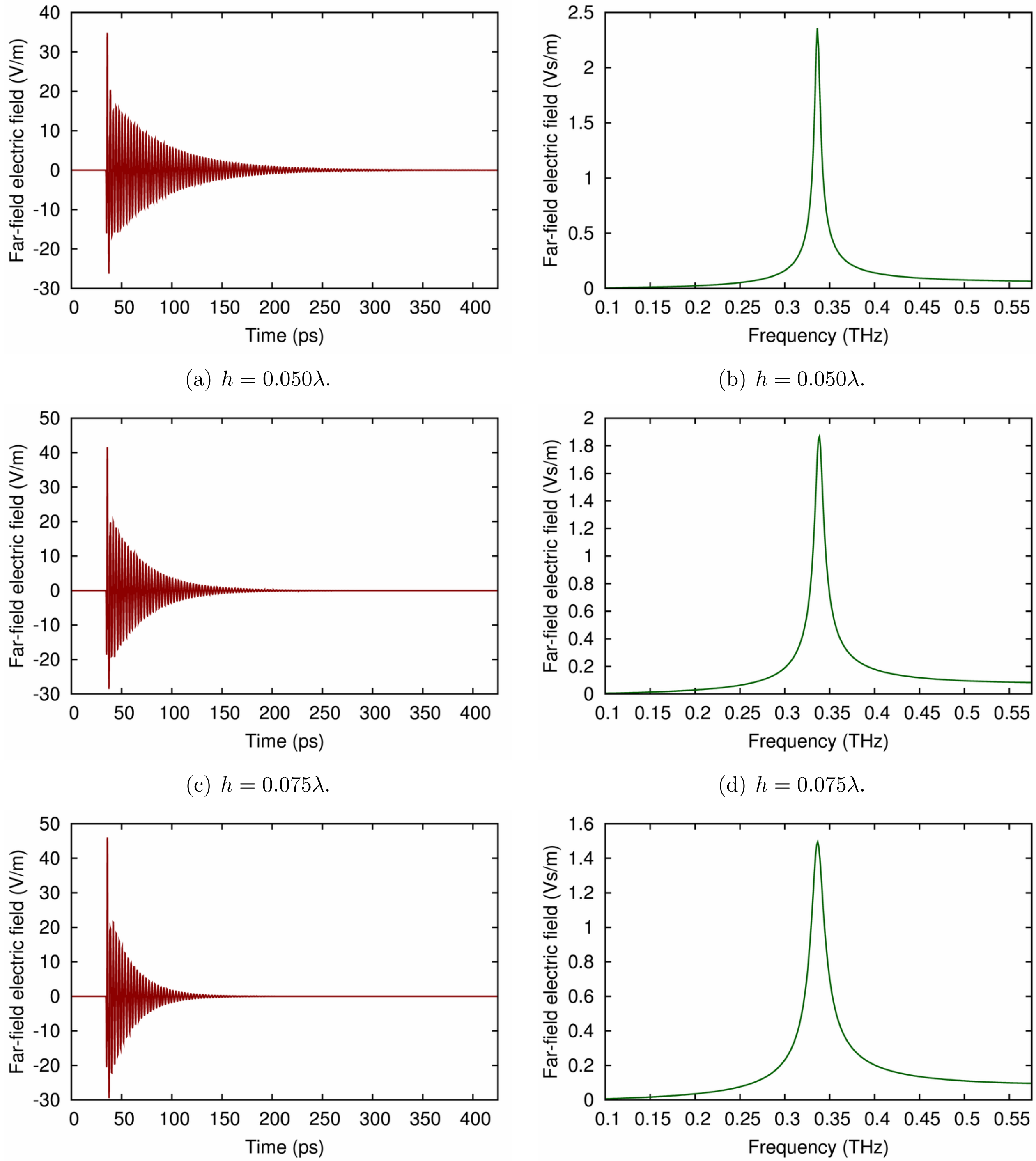

(a) $h = 0.050\lambda$.

(b) $h = 0.050\lambda$.

(c) $h = 0.075\lambda$.

(d) $h = 0.075\lambda$.

(e) $h = 0.100\lambda$.

(f) $h = 0.100\lambda$.

Figure 4.1: Radiated far-field electric field pulse in the time and frequency domains for $h = 0.50\lambda, 0.075\lambda$ and $h = 0.100\lambda$.

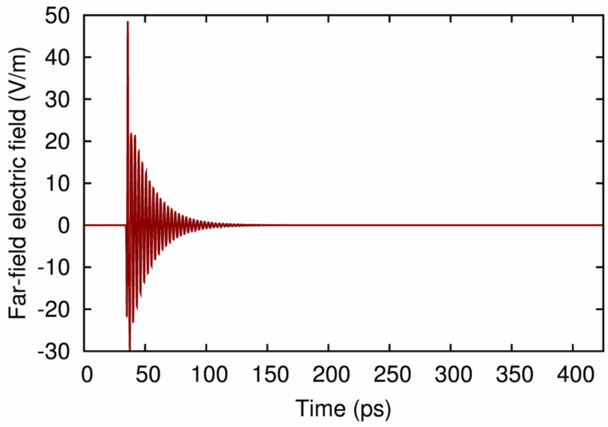

(a) $h = 0.125\lambda$.

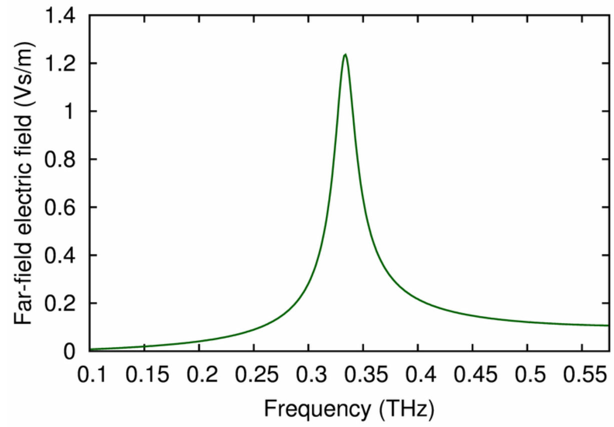

(b) $h = 0.125\lambda$.

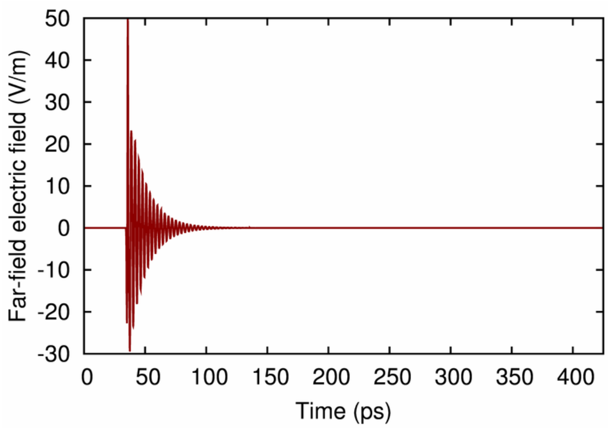

(c) $h = 0.150\lambda$.

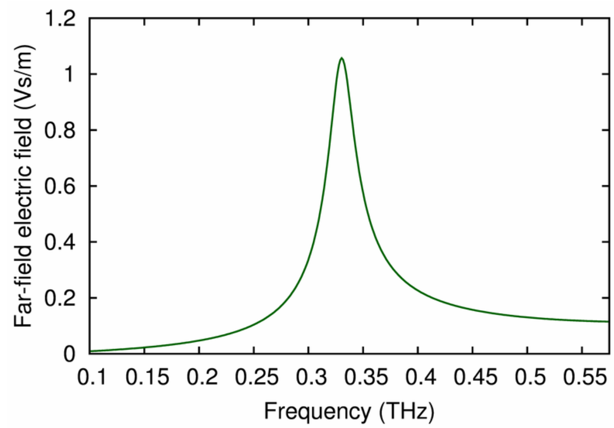

(d) $h = 0.150\lambda$.

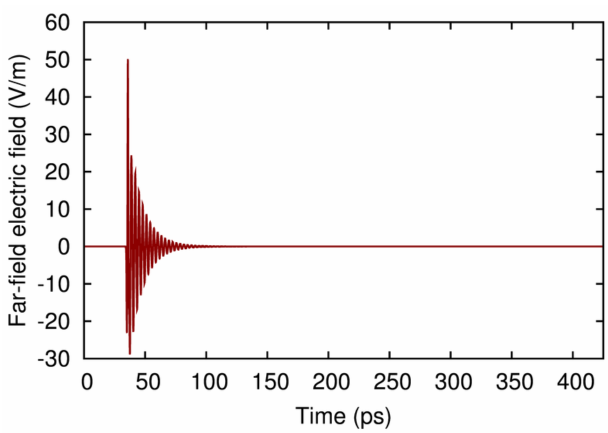

(e) $h = 0.175\lambda$.

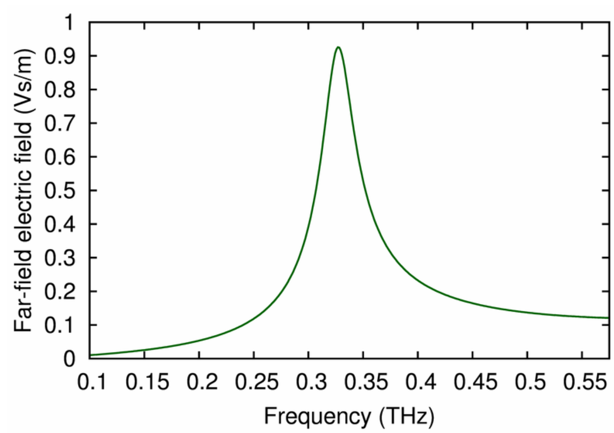

(f) $h = 0.175\lambda$.

Figure 4.2: Radiated far-field electric field pulse in the time and frequency domains for $h = 0.125\lambda, 0.150\lambda$ and $h = 0.175\lambda$.

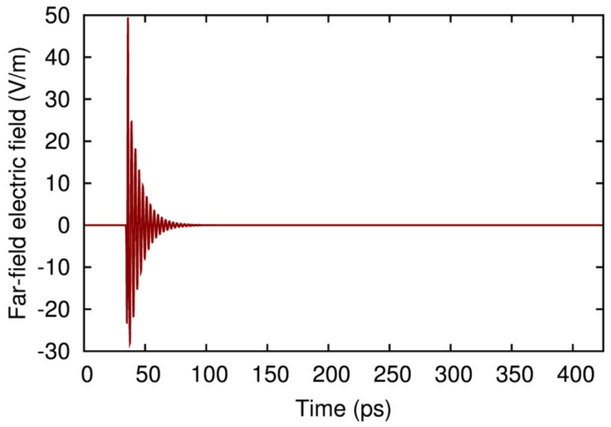

(a) $h = 0.200\lambda$.

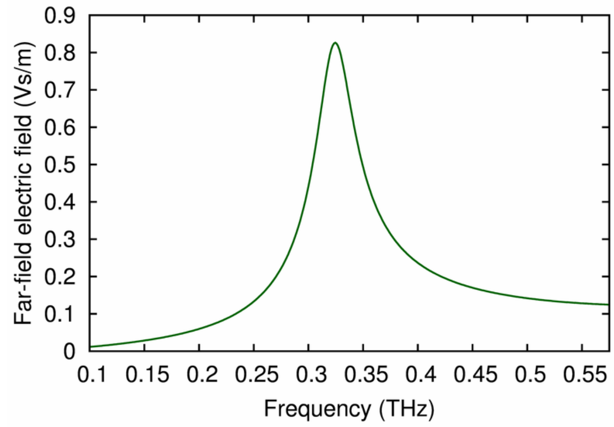

(b) $h = 0.200\lambda$.

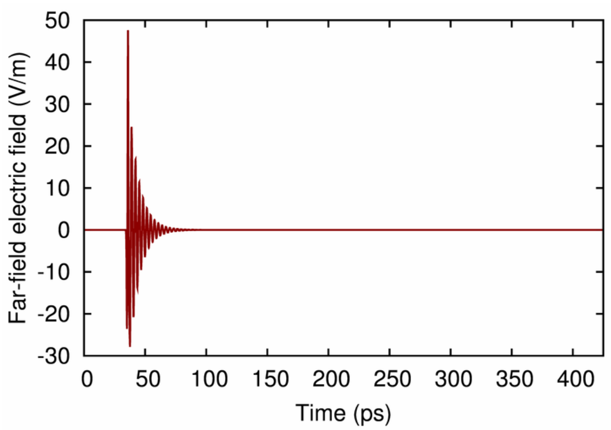

(c) $h = 0.225\lambda$.

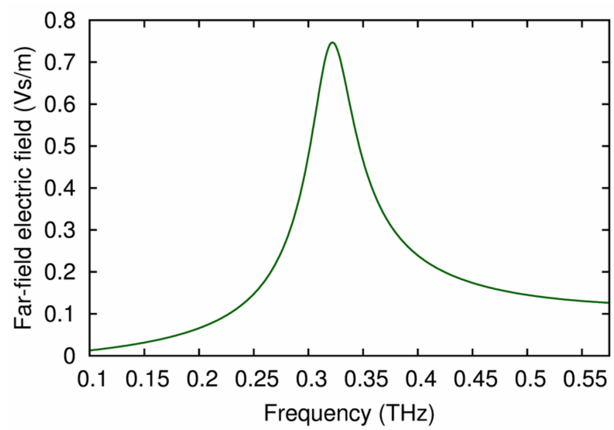

(d) $h = 0.225\lambda$.

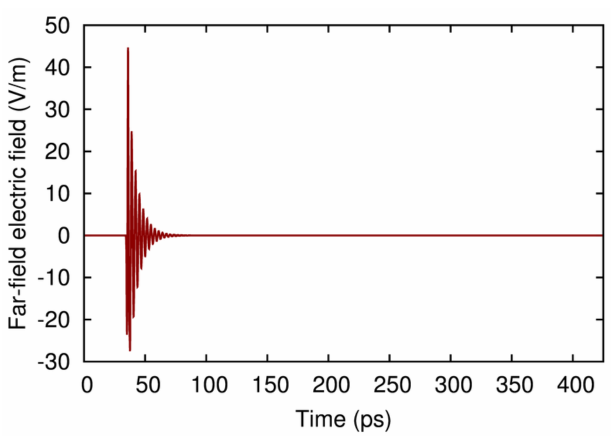

(e) $h = 0.250\lambda$.

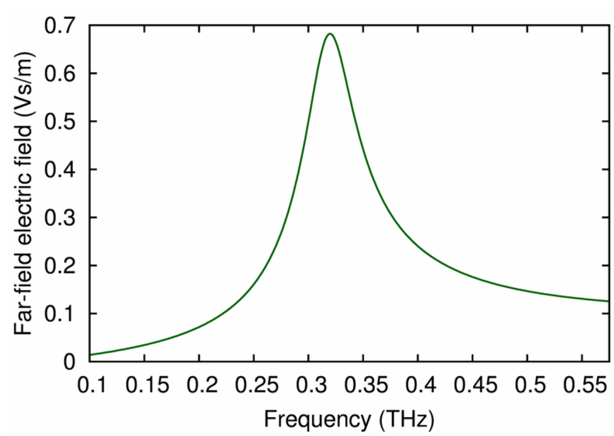

(f) $h = 0.250\lambda$.

Figure 4.3: Radiated far-field electric field pulse in the time and frequency domains for $h = 0.200\lambda, 0.225\lambda$ and $h = 0.250\lambda$.